Spatially-localized correlation of dGEMRIC-measured GAG distribution and mechanical stiffness in the human tibial plateau

Joseph T. Samosky [a,b,c], Deborah Burstein [a,d], W. Eric Grimson [b], Robert Howe [a,e], Scott Martin [f], Martha L. Gray [a,b,c,*]

[a] *Harvard-MIT Division of Health, Sciences and Technology, MIT room E25-519, Cambridge, MA 02142, USA*
[b] *Department of Electrical Engineering and Computer Science, Massachusetts Institute of Technology (MIT), Cambridge, MA 02142, USA*
[c] *New-England Baptist Bone and Joint Institute, Boston, MA, USA*
[d] *Department of Radiology, Beth Israel Deaconess Medical Center, Boston, MA, USA*
[e] *Division of Engineering and Applied Sciences, Harvard University, Cambridge, MA, USA*
[f] *Department of Orthopaedic Surgery, Brigham and Womens Hospital, Boston, MA, USA*

Abstract

The concentration of glycosaminoglycan (GAG) in articular cartilage is known to be an important determinant of tissue mechanical properties based on numerous studies relating bulk GAG and mechanical properties. To date limited information exists regarding the relationship between GAG and mechanical properties on a spatially-localized basis in intact samples of native tissue. This relation can now be explored by using delayed gadolinium-enhanced MRI of cartilage (dGEMRIC—a recently available non-destructive magnetic resonance imaging method for measuring glycosaminoglycan concentration) combined with non-destructive mechanical indentation testing. In this study, three tibial plateaus from patients undergoing total knee arthroplasty were imaged by dGEMRIC. At 33–44 test locations for each tibial plateau, the load response to focal indentation was measured as an index of cartilage stiffness. Overall, a high correlation was found between the dGEMRIC index ($T_{1_{Gd}}$) and local stiffness (Pearson correlation coefficients $r = 0.90, 0.64, 0.81$; $p < 0.0001$) when the GAG at each test location was averaged over a depth of tissue comparable to that affected by the indentation. When GAG was averaged over larger depths, the correlations were generally lower. In addition, the correlations improved when the central and peripheral (submeniscal) areas of the tibial plateau were analyzed separately, suggesting that a factor other than GAG concentration is also contributing to indentation stiffness. The results demonstrate the importance of MRI in yielding spatial localization of GAG concentration in the evaluation of cartilage mechanical properties when heterogeneous samples are involved and suggest the possibility that the evaluation of mechanical properties may be improved further by adding other MRI parameters sensitive to the collagen component of cartilage.
© 2004 Orthopaedic Research Society. Published by Elsevier Ltd. All rights reserved.

Keywords: Indentation testing; Magnetic resonance imaging; Glycosaminoglycans; Cartilage biomechanics; Tibial plateau

Introduction

The past decade has seen tremendous growth in efforts to establish non-invasive assessments of articular cartilage. These efforts are motivated by a compelling need to visualize cartilage features that are affected by disease or injury and that are expected to be modified by therapeutic strategies. Magnetic resonance imaging (MRI) approaches have emerged as the preferred means of imaging cartilage anatomy [10,13,35,36], and numerous techniques are under development for the MRI assessment of cartilage biochemical properties [7,12,14,18,40,45].

Though anatomy and biochemistry of cartilage are undeniably important metrics, the functional integrity of the tissue is reflected in its mechanical properties. Therefore significant efforts have been made to relate

---

* Corresponding author. Address: Harvard-MIT Division of Health, Sciences and Technology, MIT room E25-519, Cambridge, MA 02142, USA. Tel.: +1-617-258-8974; fax: +1-617-253-7498.
E-mail address: mgray@mit.edu (M.L. Gray).

biomechanical and biochemical properties. Abundant ex-vivo studies have shown that the load-bearing capacity of cartilage is dependent on the glycosaminoglycan (GAG) content. The structure–function relationship between GAG composition and mechanical properties has been observed in numerous studies examining normal, diseased, and experimentally-manipulated cartilages from humans and other species [1,2,15,19,20,22–25,30, 37,41], although in some studies the relationship was not as clear [5,16]. Taken together, these past studies indicate a generally strong correspondence between *bulk* tissue GAG and mechanical properties, with most of the studies involving homogeneous normal cartilage samples or homogeneously-degraded cartilage samples, and all depended on bulk assays to provide the biochemical correlate.

However, arthritis results in a spatially-heterogeneous distribution of GAG, motivating the need for spatially-localized GAG and mechanical measurements. GAG concentration can now be measured non-destructively and locally. In particular, a non-destructive image of GAG concentration can be obtained using a recently-developed charge-based MR method [8]. This method relies on the spatial distribution of the anionic paramagnetic MRI contrast agent gadolinium diethylene triamine pentaacetic acid $(Gd(DTPA)^{2-})$, which distributes within the tissue in inverse relation to the concentration of the negatively-charged sulfated GAG. Using well established biophysical relationships, the relaxation time $T_{1_{Gd}}$ (defined below) measured by MRI can be used to compute the concentration of $Gd(DTPA)^{2-}$, which in turn can be used to compute the GAG concentration ([GAG]). This method, which has been validated against biochemical and histological measures and has been successfully implemented both in vitro and in vivo [8], is referred to as dGEMRIC: delayed Gadolinium-Enhanced MRI of Cartilage ("delayed" since the method depends on having full penetration of $Gd(DTPA)^{2-}$ into the tissue and therefore requires a delay between the time the tissue is first exposed to the contrast agent and the time imaging is done).

The goal of the current study was to examine the relationship between localized measures of GAG concentration and localized measures of tissue biomechanical properties in intact human cartilage samples obtained from total knee arthroplasties. In particular, localized stiffness as measured by mechanical indentation was correlated with a co-localized index of GAG measured by dGEMRIC. We further took advantage of the spatial information provided by MRI to examine whether the correlations using full-depth measures of GAG (as would normally be used for biochemical measurements) were similar to or different from correlations using GAG measured over the depth corresponding with the volume of tissue probed mechanically.

Methods

Tissue harvest and sample preparation

Human tibial plateaus were obtained from patients undergoing total knee replacement surgery. The specimens were immediately cleaned of remaining capsular or ligamentous soft tissue and frozen until testing. One sample (HT11A) was scanned and mechanically tested without prior or intervening freezing. All procedures abided by the normal human studies regulations, including approvals from our institutional IRBs. A total of three plateaus were studied: HT3A (from a 62 year old patient), HT6A (78 years) and HT11A (81 years).

In each of the three, the medial plateau and small areas on the lateral plateau had to be excluded due to severe degeneration or fissures in the cartilage surface. Rectangular regions of visibly-intact surface amenable for study, approximately 21 mm long by 15 mm wide, were cut from the plateaus, creating osteochondral samples including about 3–5 mm of subchondral bone. These samples were mounted on acrylic registration plates (see below) with epoxy cement. All exposed bone surfaces were sealed with epoxy (Devcon 5-min epoxy; Devcon, Danvers, MA) to minimize the release of serum proteases from the bone marrow. Several investigators have reported that freezing at −20 °C does not affect the material properties of cartilage [4,26,31]. We obtained reproducibility of mechanical measurements within ±8% on average even with repeated freeze-thaw cycles and with up to a three month interval between tests [38].

A registration plate provided rigid sample fixation and a grid of fiducial marks. The MR scans were oriented so that each image included both a cross-section of the tissue sample and a subset of the marks, which were small dimples in the registration plate made MR lucent by filling them with $Gd(DTPA)^{2-}$ in agarose gel. The marks were asymmetrically distributed to allow unambiguous identification of slice number and orientation on the MR scans. A peripheral marker hole, outside the border of the sample, served as an origin to establish a coordinate frame for mechanical testing that could be directly registered with the MR coordinate frame [38].

MR imaging

The dGEMRIC protocol was used to provide an index of [GAG] from T_1 images of tissue equilibrated in $Gd(DTPA)^{2-}$. Specifically, each sample, attached to its registration frame, was entirely immersed in a minimum of 500 ml of 2 mM $Gd(DTPA)^{2-}$ (Magnevist; Berlex Laboratories, Wayne, NJ) in Hanks Balanced Salt Solution (Gibco BRL Life Technologies, Grand Island, NY) and equilibrated with continual stirring for a minimum of 12 h at 4 °C. The entire frame was then wrapped to prevent sample dehydration, placed in a 25 mm RF coil, and imaged using an 8.45 T Bruker DRX MRI system (Bruker Instruments, Billerica, MA). Samples were imaged at room temperature using an inversion recovery (IR) sequence, acquiring nine images with inversion times between 20 and 1000 ms and TR of 1200 or 1500 ms. A matrix size of 256 by 256 and field of view of 2.56 cm by 2.56 cm (yielding in-plane resolution of 100 μm) with 2 averages were used. Section thickness was 1.5 mm, equal to the indenter diameter. Multiple parallel imaging sections spaced by 3 mm were taken to cover the entire sample. With these parameters, total imaging experiment time was approximately 3 h.

Maps of $T_{1_{Gd}}$ (T_1 measured after equilibration with $Gd(DTPA)^{2-}$) were computed from the IR image sequences by computing the best fit of the parameters M_0, A, and T_1 to the theoretical biexponential signal recovery function at each pixel position:

$$s(M_0, A, T_1, TI, TR) = |M_0(1 - 2Ae^{(-TI/T_1)} + e^{(-TR/T_1)})|$$

where s is the measured MRI signal intensity (i.e., the pixel intensity in the IR image), T_1 is the spin–lattice relaxation time which we wish to estimate, M_0 is proportional to the proton density, A is a constant related to experimental conditions, TI is the inversion time used for the image, and TR is the repeat time (a constant for all images in a given study).

GAG concentration maps were calculated from the $T_{1_{Gd}}$ maps according to previously-validated equations [6]. For these calculations, $T_{1_{tissue}}$ (T_1 in the absence of $Gd(DTPA)^{2-}$) was assumed to be uniformly equal to 1.7 s, and relaxivity, r, uniformly equal to 4.5 $(mM\,s)^{-1}$. We have previously reported that at 8.45 T, $T_{1_{tissue}}$ in native and trypsin-

depleted bovine cartilage ranges from 1.57 to 1.88 s, and r ranges from 4.18 to 4.5 $(\text{mM s})^{-1}$ [17]. With this range of variability, the error incurred in computing $Gd(DTPA)^{2-}$ by assuming a constant $T_{1_{tissue}}$ is $\pm 2\%$; the error incurred by assuming a constant r is $+8\%$ to -4%. This degree of potential error was considered acceptable for this initial study.

Mechanical indentation testing

To obtain an index of mechanical properties, the cartilage was indented at a regularly-spaced array of locations using a custom-built, precision compression testing apparatus. This mechanical spectrometer provided computer-controlled vertical (z-axis) displacement of an indenter (positional accuracy 1 μm) while continuously measuring in-line load (0.1 g resolution).

We chose to match the geometry of a standard arthroscopic probe tip by utilizing a rigid, non-porous, hemispherically-tipped indenter with a diameter of 1.5 mm. The indenter was positioned at target locations on the sample surface by vertical (z-axis) displacement of the indenter and horizontal (x, y-axis) translation of the sample with a two-axis linear translation stage. Positioning accuracies and repeatability were typically ± 10 μm [38], which is well under the dimension of a pixel (100 μm) in the MR images.

At the time of mechanical testing, the sample and registration plate were attached to the bottom of a polycarbonate hydration tank filled with Hank's solution. For each measurement, the indenter was positioned above the desired test location and then slowly lowered at a rate of 10 μm/s until a tare load of 1 g was reached. The indenter was then displaced into the cartilage surface with a half cycle of a 0.25 Hz sinusoidal displacement waveform to a peak amplitude of 300 μm. The resulting peak load was measured and used as a measure of mechanical stiffness. All test sites were at least 2.25 mm from the edge of the specimen (a minimum of approximately four times the indenter-tissue contact radius at maximum indentation). These tibial plateau samples were all relatively flat, so that a single positioning of the sample to be visually perpendicular to the indenter served for all test sites. For one sample, multiple sites were tested on three separate occasions over three months by two independent operators; agreement in measured peak loads across all locations tested was, on average, within 8%, suggesting that this protocol is quite robust and that the sample preparation and storage methods preserved mechanical integrity over time [38]. With this displacement amplitude, estimated peak stresses were always under 4 MPa.

Apparent indentation stiffness (i.e. the ratio of measured load to indentation depth) depends on cartilage thickness, with apparent stiffness increasing with thinner tissue. Various models of indentation [21,28,29,38] have shown that apparent stiffness increases dramatically when cartilage thickness is less than the indenter diameter. Consistent with those reports, a finite-element analysis we conducted for the specific parameters of our study (300 μm displacement of a 1.5 mm diameter spherically-tipped indenter) indicated that the apparent stiffness varies by less than $\pm 10\%$ with variation in cartilage thickness between 2 and 5 mm [38]. By comparison, at 1 mm thickness the apparent stiffness increases by approximately 50% compared to a 2 mm thick layer. The median cartilage thickness at loci tested in the present study was 2.5 mm, with a range of 1.4–4.2 mm, with over 80% of the test sites having cartilage thickness greater than 2 mm, suggesting that effects of thickness variations on apparent stiffness were likely to be minimal in the present study. To confirm this, analysis was also done after excluding all loci having cartilage thickness less than 2 mm.

Computing an index of [GAG] at the test loci

To establish an index of cartilage [GAG] at each indentation site, $T_{1_{Gd}}$ was averaged over a region of interest (ROI) that corresponded with each indentation site. Specifically, pixels underneath the indenter and to a depth of twice the indentation depth (corresponding to a square column, 1.5 mm by 1.5 mm, 600 μm deep) were included in the average for a site. This served as a first-order approximation of the tissue most directly "sensed" by the mechanical probe. In support of this selection of a sensing volume, we computed that VonMises stress under the indenter is estimated to drop by about 50% at a depth of twice the indentation [38].

Quantifying the relationship between MRI and mechanical indices: statistical analysis

Correlation between $T_{1_{Gd}}$ averaged over the ROIs and the peak load responses was evaluated statistically using the Pearson correlation test. This analysis was done: (i) for full data sets from each plateau, (ii) for the combined data from all three tibial plateaus, and (iii) for two functionally-distinct regions in each plateau (the peripheral region normally covered by the meniscus and the uncovered central region). For analysis (iii), we categorized test loci as "submensical" or "central" only if they were unambiguously in the respective region; test locations near the border of the meniscus were excluded. For each correlation test, statistical significance was determined from a t-test, with a null hypothesis that the Pearson correlation equals 0; p-values of less than 0.05 were considered significant. The slopes of the linear regressions for data from different plateaus were compared using analysis of covariance to compute the F statistic.

Results

A total of 119 test sites from three tibial plateaus were measured both mechanically and by dGEMRIC. Across all samples and loci tested, peak load responses ranged from 20 g to approximately 500 g. For the indenter geometry and indentation depth employed, the contact area was about 1.4 mm^2, yielding an estimated applied stress ranging from 140 kPa to 3.5 MPa. For comparison to other studies, the range of load responses we observed corresponds to an approximate elastic modulus range of 0.6 MPa to 14 MPa, determined from a finite element model with the indenter geometry and depth employed and under the assumptions of cartilage elasticity, homogeneity, isotropy, and Poisson's ratio v near 0.5 [38]. Locally-averaged $T_{1_{Gd}}$ at the sites of indentation ranged from 101 to 203 ms, which corresponds to a range of local [GAG] of 0 mg/ml to 53 mg/ml.

To appreciate the comparison between dGEMRIC and mechanical data, consider three separate image slices from one sample and their corresponding mechanical stiffness profiles (Fig. 1). The three sections of this sample demonstrate three different patterns of [GAG] and stiffness variation: a focal area of deficit, a region of relatively uniform [GAG], and a region in which [GAG] increases from one end of the sample to the other. In each case, a correlated pattern of load response (i.e., stiffness) variation and locally-averaged [GAG] variation is evident across the 11 colinear loci of each slice. In particular, the sensitivity of the test methodology to the presence of a focal lesion is demonstrated in Figs. 1a and d. Here, a focal area of [GAG] depletion, evident in both the [GAG] map (Fig. 1a) and the corresponding locally-averaged [GAG] profile (Fig. 1d), is associated with a correlated pattern of reduction in peak load response (Fig. 1d).

When data from all loci on a given sample were considered, the load response (and therefore stiffness) was found to be strongly correlated with locally-averaged $T_{1_{Gd}}$, with Pearson correlation coefficients of 0.90,
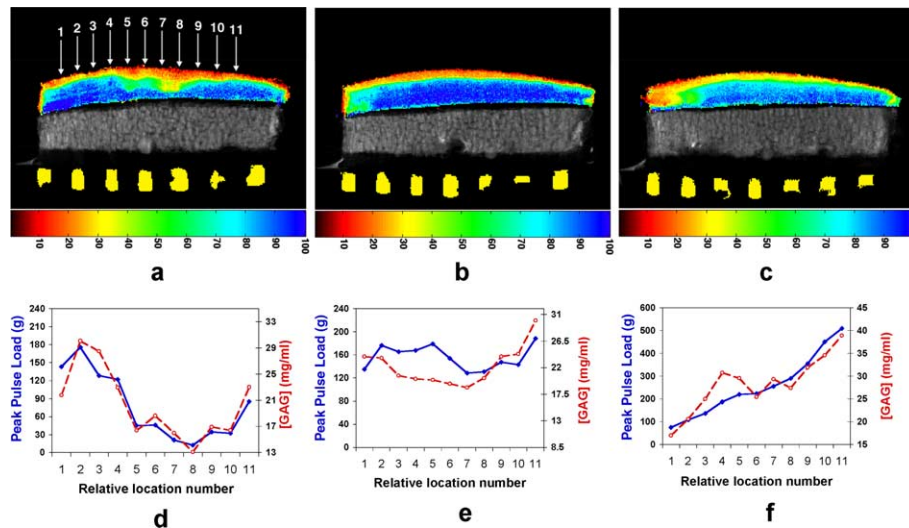
Fig. 1. (a)–(c) [GAG] maps of three adjacent sections of human tibial plateau (sample HT3A). Color map of the cartilage shows distribution of [GAG] (mg/ml). The numbered arrows in (a) show the positions of 11 loci where stiffness measurements were performed. Similar sets of loci are defined for (b) and (c). MRI-lucent registration markers in the registration plate are visible beneath each sample. Loci and adjacent sections are spaced by 3 mm. In (a), an area of relative GAG depletion can be seen extending from locus 5 to locus 10. (d)–(f): Peak load responses (solid blue curves) and locally-averaged [GAG] values (dotted red curves; 600 μm depth of averaging) show similar variation across the 11 colinear locations in each slice. Especially noticeable are the focal reduction in both load response and [GAG] between loci 5 and 10 in (d), the relatively smaller variation of both load response and [GAG] across most loci in (e), and the approximately steady increase in both indices across the loci in (f).

0.64, and 0.81, respectively ($p < 0.0001$ for each, Fig. 2). Although the intercepts were not the same, ANCOVA analysis of the homogeneity of the slopes indicated that the slopes were not significantly different ($F = 1.188$, $p = 0.31$). When all loci from the three samples were considered together, the Pearson correlation coefficient was 0.56 ($p < 0.0001$).

To assess the potential effect of cartilage thickness on load response for the present study, we repeated the analysis of correlation between stiffness and T_{1Gd} after excluding all loci with thickness under 2 mm. The correlations remained high at 0.81, 0.69, and 0.80 ($p < 0.0001$), with no significant effect on the slopes of the regression lines.

While the results reported here averaged T_{1Gd} over the volume expected to be "sensed" by the mechanical probing protocol, analyses were also done for T_{1Gd} averaged over both shallower and deeper regions-of-interest (ROIs) of tissue (Fig. 3). For sites from two of the tibial plateaus (HT6A and HT11A), the correlation between stiffness and T_{1Gd} decreased as averaging depth increased beyond about 700 μm (correlation was essentially the same for averaging depths from 100 to 700 μm). The effect of depth of T_{1Gd} averaging on the correlation between stiffness and average T_{1Gd} varied from section to section. Full analysis of the effect of different ROI depths on the correlation between stiffness and T_{1Gd} or [GAG] was beyond the scope of this study; the objective here was to evaluate the importance of averaging the index of [GAG] over variable-depth ROIs versus averaging over the full depth, as is normally done for destructive biochemical analyses.

The correlation analyses above combined data from all areas of a specimen. To compare functionally-distinct regions, we separately examined data for test sites in the submeniscal and central regions of each sample. The average peak load response was significantly higher for loci in the submeniscal region of each sample (170%, 560%, 540% for HT3A, HT6A and HT11A, respectively; $p < 0.001$ for each sample) than for loci in the central region (Fig. 4a). Similarly, the average T_{1Gd} (or [GAG]) of loci in the submeniscal region was higher (14.6%, 9.3%, 27.2%; $p < 0.003$ for each sample) than for loci in the central region (Fig. 4b). By examining the correlation between peak load and T_{1Gd} in each region (Fig. 5), we found that the submeniscal regions each showed uniformly very high correlations, with $r = 0.97$, 0.90 and 0.94 ($p < 0.0001$). The central regions also showed correlations, but the correspondence was not as strong, and for HT6A and HT11A, the slope and intercept of the regression were significantly different between the submeniscal and central regions ($p < 0.001$).

Discussion

To our knowledge, this is the first study in cartilage to closely localize a biochemical measure to the footprint of a small indenter, a capability made possible by the spatial resolution of dGEMRIC and the MRI-mechanical registration methodology employed. The general finding that a metric of GAG concentration (MR measurement of T_{1Gd}) is well correlated with a measure of

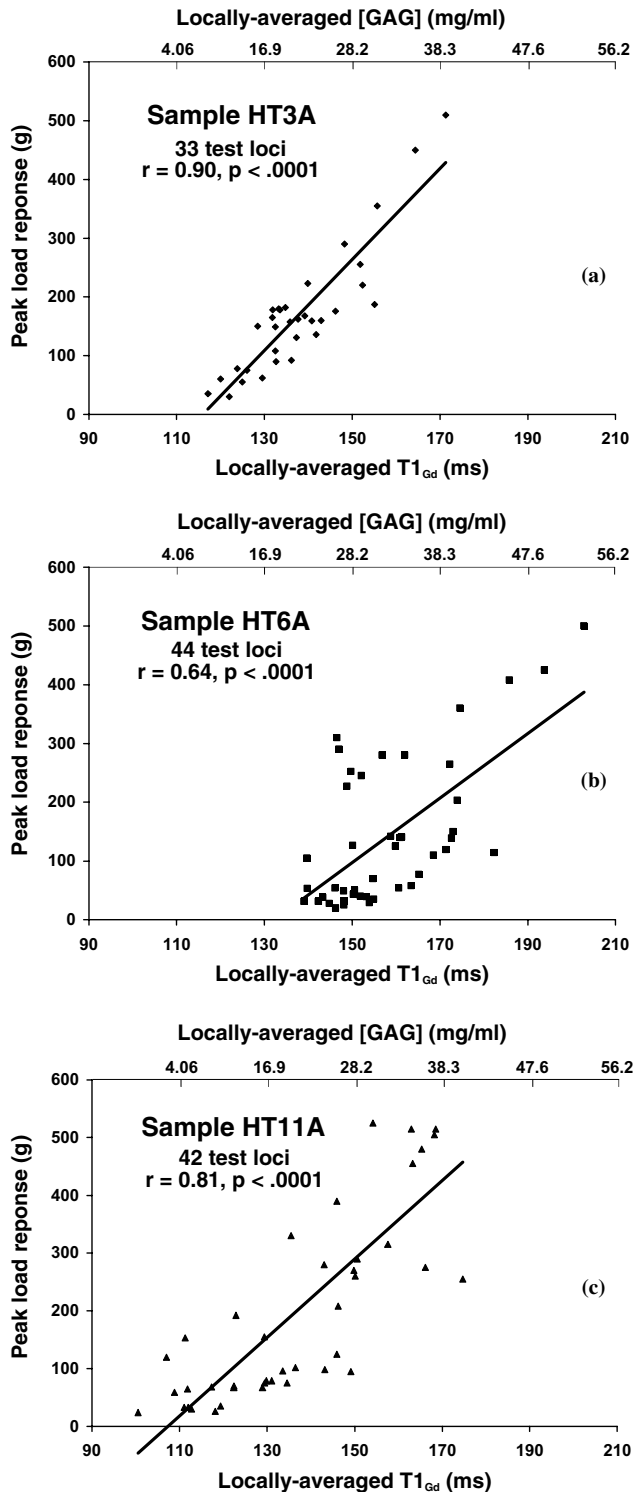Fig. 3. The correlation between load response and locally-averaged T_{1Gd} depends on the depth of the region of interest (ROI) over which T_{1Gd} is averaged. Shown here is the correlation coefficient as a function of averaging depth, computed for each tibial plateau sample (in all cases the volume of the ROI averaged at each test locus had dimensions 1.5 mm × 1.5 mm × depth from articular surface). The variation of correlation with averaging depth is least pronounced for HT3A, the sample having the least depth-variation in the pattern of T_{1Gd} (and [GAG]) distribution.

Fig. 2. Peak load during indentation at the test loci, an index of cartilage stiffness, is correlated with locally-averaged T_{1Gd} and [GAG] (measured by dGEMRIC) at the loci for three different lateral tibial plateau samples. (a) HT3A, 62 year old female. (b) HT6A, 78 year old male. (c) HT11A, 81 year old female. Pearson correlation coefficients are given for the correlation of peak load response to T_{1Gd}. The intercepts differ, but the slopes of the three regression lines are not significantly different ($p = 0.31$). When data from all samples are combined (119 test loci total), the Pearson correlation coefficient is 0.56 ($p < 0.0001$).
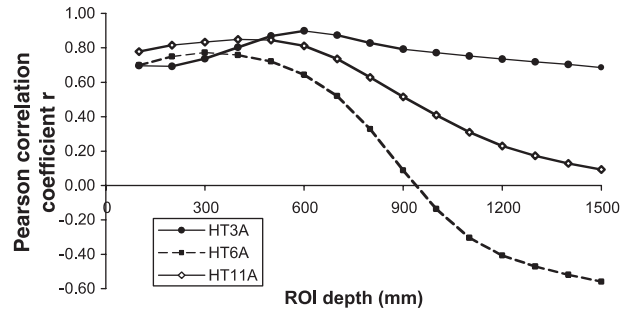
mechanical stiffness is consistent with many other reports [1,2,15,19,20,22–25,30,37,41]. More notably, our results demonstrate the importance of obtaining information about the local distribution of GAG concentration when trying to infer biomechanical tissue properties, particularly when there is significant local spatial variation in the biochemistry and biomechanics. Indeed, for sites from two of the three tibial plateaus, the correlation coefficient between stiffness and T_{1Gd} decreased dramatically as averaging depth increased beyond about 700 μm (Fig. 3). Furthermore, in two of the three tibial plateaus, when the average [GAG] was computed over the *full* thickness, the correlation between [GAG] and indentation stiffness was eliminated. This result may help explain two previous studies in which mechanical properties were found not to correlate well with GAG, studies which involved full thickness GAG analyses in human knee articular surfaces exhibiting natural variation in cartilage integrity where one would expect the potential for considerable local spatial heterogeneity [5,16].

While the MRI and indentation studies here yielded high overall correlations between [GAG] and load response, clearly other factors must be considered. First, it is certainly true that many biochemical and architectural features influence tissue stiffness, as has been suggested by previous experimental and theoretical work [3,9,27, 33,42]. Indeed, our finding that correlation increased when the peripheral (submeniscal) and central regions were evaluated separately is a direct indication that factors in addition to GAG are significantly influencing the mechanical properties. Previous EM studies revealed distinct differences in collagen fiber arrangement between the central and submeniscal regions [11]. Such regional differences in collagen architecture would be expected to be reflected in commensurate differences in
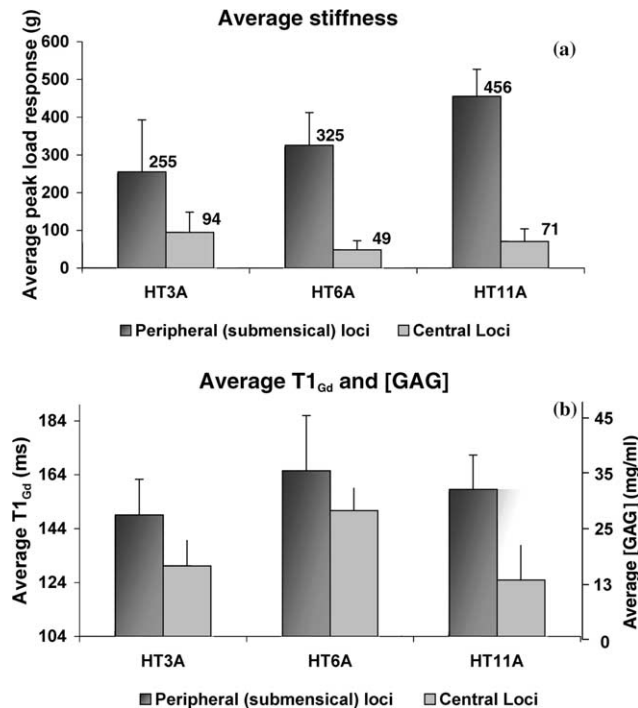
Fig. 4. Submeniscal-central regional differences in average stiffness and average $T_{1_{Gd}}$ and [GAG] for each of three tibial plateau samples. (a) The average indentation load response (an index of stiffness) for loci in the submeniscal region is 2.7 (HT3A) to 6.6 (HT6A) times higher than the average load response of loci in the central region. Error bars indicate standard deviation. (b) The average $T_{1_{Gd}}$ and [GAG] are also significantly higher in the submeniscal region ($p < 0.003$ for each sample) than in the central region.

measured mechanical stiffness since the focal indentation used in the current study induces both tensile and compressive stresses and collagen architecture influences the tensile behavior.

This issue also suggests the attractive possibility of combining MRI techniques sensitive to GAG and collagen to offer an even more robust, tightly-bound prediction of cartilage compressive load response and to enable further enhanced non-invasive mapping of the mechanical stiffness of the articular surface. A few studies have examined the relationship between the MRI parameter T2 and mechanical properties. In one study, T2 for native and enzymatically-treated porcine cartilage correlated ($r^2 = 0.51$) with the aggregate modulus [43]. However, that same study also found a strong correlation between GAG content and aggregate modulus ($r^2 = 0.89$) and between T2 and GAG content ($r^2 = 0.44$), raising the question of whether the correspondence between T2 and modulus could be explained by [GAG]. The conclusions were slightly different in another study involving native and enzymatically-treated bovine humeral head cartilage, where the observed relationship between T2 relaxation and Young's modulus was non-monotonic, with T2 being relatively insensitive to the substantial changes in mod-

ulus induced by GAG depletion and very sensitive to the modest changes in modulus induced by exposure to collagenase [34]. Although the biophysical basis for T2 is unclear, as is its relationship to mechanical properties, there is evidence that T2 provides information that is independent of that provided by dGEMRIC (i.e., differences in T2 do not correspond to differences in $T_{1_{Gd}}$) [32]. Thus, T2 in conjunction with dGEMRIC as a means of establishing a metric that is predictive of mechanical properties is a clear direction for further research.

Additional metrics of tissue biochemistry may also help explain why the correlation between stiffness and local GAG concentration decreased when data from all samples were pooled together. While the high correlation within a given sample should allow determination of relative stiffness within an area of a sample, the additional metrics may allow for an absolute level of stiffness to be determined from imaging data, permitting meaningful between-sample comparisons.

Another advantage of MRI-based methods is the possibility of measuring and potentially accounting for local tissue thickness, a factor which could influence the interpretation of the mechanical measurements. With regard to tissue thickness, theoretical analyses by us and other groups have concluded that for thickness sufficiently larger than the indenter contact radius, thickness effects are small [21,28,29,38]. These analyses assumed a rigid indenter pressing into an isotropic linear elastic layer adhered to a rigid substrate. Specifically, these studies collectively indicate that, for our indenter geometry and displacement depth, the influence of cartilage thickness on stiffness measurements is small (20% or less) when cartilage thickness is $\geqslant 2$ mm. Over 80% of the loci in the present study were $\geqslant 2$ mm thick and, when only those samples were included in the analysis, the regression between load response and $T_{1_{Gd}}$ was statistically unchanged. This result suggests that for these joint samples thickness was not a prominent confounding factor and certainly not one that could explain the 500% variation in stiffness for our samples. However, the ability to measure the local cartilage thickness does allow for this factor to be taken into account in the future if samples contain a higher degree of thickness variation.

The choice of loading rate also impacts the interpretation of the mechanical testing. The frequency-dependent stress/strain profiles in cartilage may have a frequency-dependent correspondence to [GAG]. A systematic comparison of the mechanical frequency response with [GAG] may provide additional insight into the role of GAG macromolecules in different regimes of mechanical behavior.

An additional advantage of MRI is the potential to use the imaging metrics to obtain a topographical map of tissue properties across the cartilage surface. This
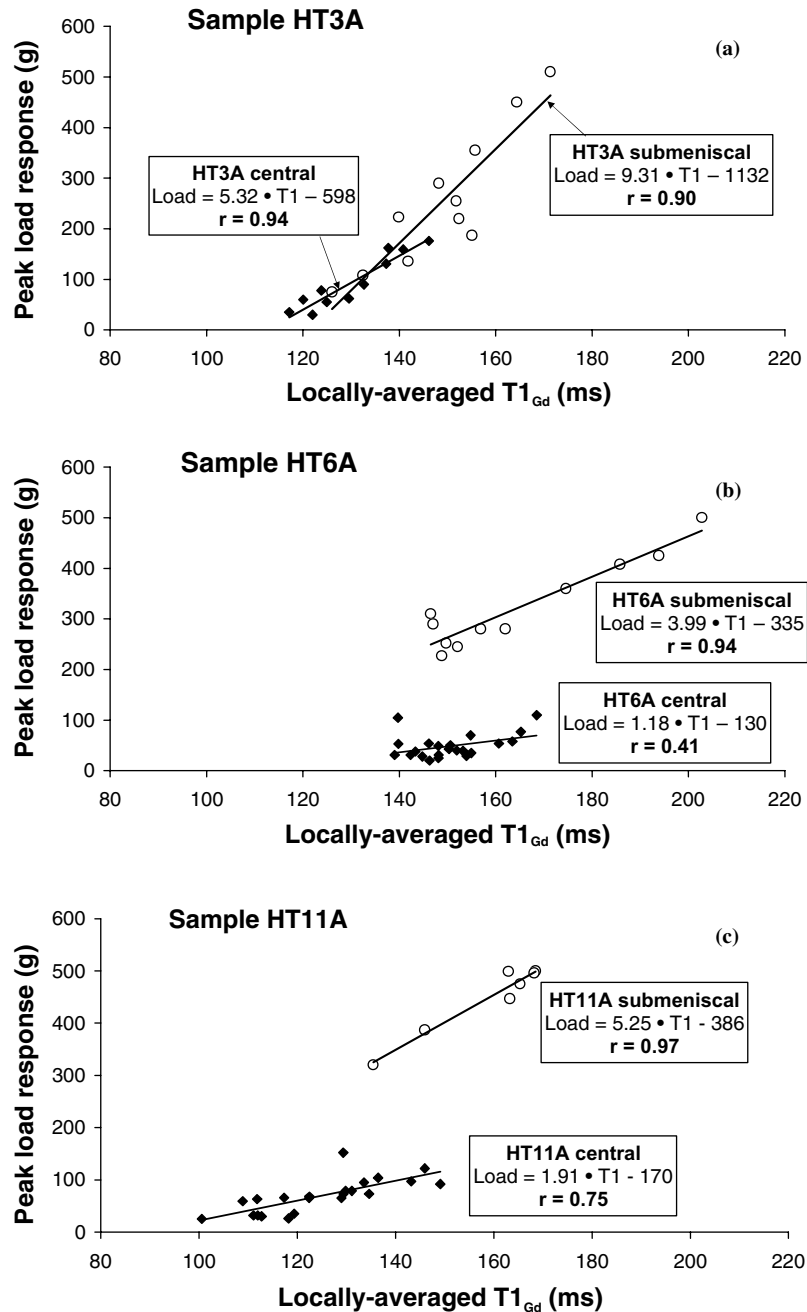
Fig. 5. Data of Fig. 2 reanalyzed after partitioning loci in accordance with their spatial location: submeniscal and central (loci that were located at the interface between the regions were not included in the analysis). All other details are the same as described in Fig. 2. (a) HT3A, 62 year old female. (b) HT6A, 78 year old male. (c) HT11A, 81 year old female. The submeniscal loci exhibit uniformly high correlations between load response and locally-averaged $T_{1_{Gd}}$. The central regions also exhibit significant correlations, but with more variability between samples. For samples HT6A and HT11A, the load/$T_{1_{Gd}}$ relationship (as reflected by the slope) is different in the central region compared with the submeniscal region. p value for the difference in submeniscal versus central slopes equals 0.051, 0.0012 and 0.0002 for HT3A, HT6A and HT11A, respectively. Sample HT3A, for which the slopes were statistically the same between the two regions, also exhibited the least frank variation in the appearance of the articular surface.

concept is illustrated in Fig. 6 for an osteochondral sample, showing the close qualitative similarity between a topographical map based on indentation information and one based on a synthesis of the depth-averaged GAG concentration obtained from dGEMRIC imaging data. With further advances in the ability to infer local-

ized mechanical properties from localized biochemical properties, such a topographical map could, in principle, quickly reveal the distribution of mechanically competent or incompetent cartilage across an articular surface.

In principle, the clinical availability of dGEMRIC offers the possibility of performing studies such as those
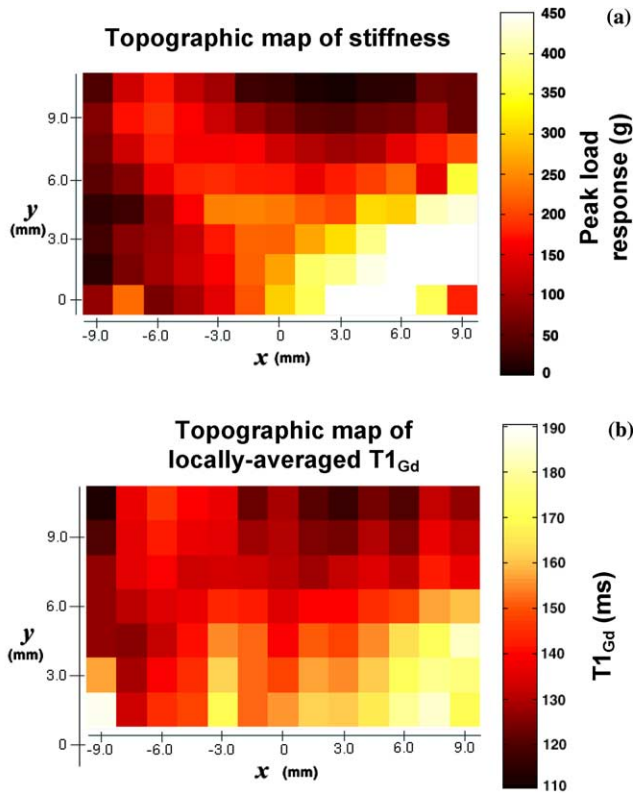
Fig. 6. A potential use of MR-derived mechanical metrics is the creation of topographical maps with color indicating localized mechanical properties. This concept is illustrated by comparison of two ''views'' of the articular surface of an osteochondral sample—one derived from direct mechanical measurements and the other derived from a dGEMRIC image dataset. (a) Topographic map of cartilage stiffness in which color indicates peak indentation load (g) measured (as described in methods) in the center of each 1.5 mm by 1.5 mm location. (b) Topographic map computed from a set of dGEMRIC images of the same sample. Each location corresponds spatially to the mechanical map of (a) and is colored according to an estimate of locally-averaged $T_{1_{Gd}}$, averaged over the same 1.5 mm by 1.5 mm area and to a depth of 600 μm. The averaged-$T_{1_{Gd}}$ map shows generally similar spatial variation to the stiffness map: in particular, areas of softening seen at the top and left edge of the stiffness map correspond to areas of relatively lower T_1 in the $T_{1_{Gd}}$ map. In addition, the cartilage is seen to be stiffest toward the lower right corner of the specimen, and this area also exhibits high $T_{1_{Gd}}$ (and hence high [GAG]).

described here in vivo. A recent study demonstrated that arthroscopically-diagnosed diseased compartments had lower dGEMRIC indices overall than the reference compartments [39]. The current resolution of clinical dGEMRIC images is typically on the order of 300 μm in-plane resolution with a 2–3 mm section thickness, and significant spatial heterogeneity of the dGEMRIC index is apparent in clinical images with this resolution [44]. The possibility of obtaining an in vivo measure of the relative mechanical status of cartilage throughout the joint by dGEMRIC alone or in combination with other non-invasive MRI measures makes further studies in this area compelling.

References

[1] Allen RG. Mechanical properties of selectively degraded cartilage explants: correlation to the spatiotemporal distribution of glycosaminoglycans. In: Mechanical engineering. Cambridge: Massachusetts Institute of Technology; 1996.

[2] Armstrong CG, Mow VC. Variations in the intrinsic mechanical properties of human articular cartilage with age, degeneration, and water content. J Bone Jnt Surg Am 1982;64:88–94.

[3] Askew MJ, Mow VC. The biomechanical function of the collagen fibril ultrastructure of articular cartilage. J Biomech Eng 1978; 100:105–15.

[4] Athanasiou KA, Rosenwasser MP, Buckwalter JA, Malinin TI, Mow VC. Interspecies comparisons of in situ intrinsic mechanical properties of distal femoral cartilage. J Orthop Res 1991;9:330–40.

[5] Bae WC, Temple MM, Rivard KL, Niederauer G, Sah RL. Indentation testing of human articular cartilage: sensitivity to indices of degeneration. In: Trans Orthop Res Soc, Dallas, TX, 2002. p. 252.

[6] Bashir A, Gray ML, Burstein D. Gd-DTPA2⁻ as a measure of cartilage degradation. Magn Reson Med 1996;36:665–73.

[7] Burstein D, Bashir A, Gray ML. MRI techniques in early stages of cartilage disease. Invest Radiol 2000;35:622–38.

[8] Burstein D, Gray ML. Potential of molecular imaging of cartilage. Sports Medicine Arthrosc Rev 2003;11:182–91.

[9] Chen SS, Falcovitz YH, Schneiderman R, Maroudas A, Sah RL. Depth-dependent compressive properties of normal aged human femoral head articular cartilage: relationship to fixed charge density. Osteoarthr Cartilage 2001;9:561–9.

[10] Cicuttini F, Forbes A, Morris K, Darling S, Bailey M, Stuckey S. Gender differences in knee cartilage volume as measured by magnetic resonance imaging. Osteoarthr Cartilage 1999;7:265–71.

[11] Clark JM. Variation of collagen fiber alignment in a joint surface: a scanning electron microscope study of the tibial plateau in dog, rabbit, and man. J Orthop Res 1991;9:246–57.

[12] Duvvuri U, Goldberg AD, Kranz JK, Hoang L, Reddy R, Wehrli FW, et al. Water magnetic relaxation dispersion in biological systems: the contribution of proton exchange and implications for the noninvasive detection of cartilage degradation. Proc Natl Acad Sci USA 2001;98:12479–84.

[13] Eckstein F, Reiser M, Englmeier KH, Putz R. In vivo morphometry and functional analysis of human articular cartilage with quantitative magnetic resonance imaging—from image to data, from data to theory. Anat Embryol (Berl) 2001;203:147–73.

[14] Fragonas E, Mlynarik V, Jellus V, Micali F, Piras A, Toffanin R, et al. Correlation between biochemical composition and magnetic resonance appearance of articular cartilage. Osteoarthr Cartilage 1998;6:24–32.

[15] Frank EH, Grodzinsky AJ, Koob TJ, Eyre DR. Streaming potentials: a sensitive index of enzymatic degradation in articular cartilage. J Orthop Res 1987;5:497–508.

[16] Franz T, Hasler EM, Hagg R, Weiler C, Jakob RP, Mainil-Varlet P. In situ compressive stiffness, biochemical composition, and structural integrity of articular cartilage of the human knee joint. Osteoarthr Cartilage 2001;9:582–92.

[17] Gillis A, Gray M, Burstein D. Relaxivity and diffusion of gadolinium agents in cartilage. Magn Reson Med 2002;48:1068–71.

[18] Gray ML, Burstein D, Xia Y. Biochemical (and Functional) imaging of articular cartilage. Semin Musculoskelet Radiol 2001;5:329–44.

[19] Guilak F, Ratcliffe A, Lane N, Rosenwasser MP, Mow VC. Mechanical and biochemical changes in the superficial zone of articular cartilage in canine experimental osteoarthritis. J Orthop Res 1994;12:474–84.

[20] Harris Jr ED, Parker HG, Radin EL, Krane SM. Effects of proteolytic enzymes on structural and mechanical properties of cartilage. Arthritis Rheum 1972;15:497–503.

[21] Hayes WC, Keer LM, Herrmann G, Mockros LF. A mathematical analysis for indentation tests of articular cartilage. J Biomech 1972;5:541–51.

[22] Hoch DH, Grodzinsky AJ, Koob TJ, Albert ML, Eyre DR. Early changes in material properties of rabbit articular cartilage after meniscectomy. J Orthop Res 1983;1:4–12.

[23] Jurvelin JS, Arokoski JP, Hunziker EB, Helminen HJ. Topographical variation of the elastic properties of articular cartilage in the canine knee. J Biomech 2000;33:669–75.

[24] Kempson. Adult articular cartilage. Pitman Medical: London; 1979.

[25] Kempson GE, Muir H, Swanson SA, Freeman MA. Correlations between stiffness and the chemical constituents of cartilage on the human femoral head. Biochim Biophys Acta 1970;215:70–7.

[26] Kempson GE, Spivey CJ, Swanson SA, Freeman MA. Patterns of cartilage stiffness on normal and degenerate human femoral heads. J Biomech 1971;4:597–609.

[27] Lyyra T, Arokoski JP, Oksala N, Vihko A, Hyttinen M, Jurvelin JS, et al. Experimental validation of arthroscopic cartilage stiffness measurement using enzymatically degraded cartilage samples. Phys Med Biol 1999;44:525–35.

[28] Lyyra T, Jurvelin J, Pitkanen P, Vaatainen U, Kiviranta I. Indentation instrument for the measurement of cartilage stiffness under arthroscopic control. Med Eng Phys 1995;17:395–9.

[29] Lyyra-Laitinen T, Niinimaki M, Toyras J, Lindgren R, Kiviranta I, Jurvelin JS. Optimization of the arthroscopic indentation instrument for the measurement of thin cartilage stiffness. Phys Med Biol 1999;44:2511–24.

[30] Maroudas A. Physicochemical properties of articular cartilage. In: Freeman M, editor. Adult articular cartilage. London: Pitman; 1979. p. 215–90.

[31] Maroudas A, Bullough P, Swanson SA, Freeman MA. The permeability of articular cartilage. J Bone Jnt Surg Br 1968;50:166–77.

[32] Menezes NM, Gray ML, Hartke JR, Burstein D. T2 and T1 rho MRI in articular cartilage systems. Magn Reson Med 2004;S1:503–9.

[33] Mizrahi J, Maroudas A, Lanir Y, Ziv I, Webber TJ. The instantaneous deformation of cartilage: effects of collagen fiber orientation and osmotic stress. Biorheology 1986;23:311–30.

[34] Nieminen MT, Toyras J, Rieppo J, Hakumaki JM, Silvennoinen J, Helminen HJ, et al. Quantitative MR microscopy of enzymatically degraded articular cartilage. Magn Reson Med 2000;43:676–81.

[35] Raynauld JP, Kauffmann C, Beaudoin G, Berthiaume MJ, de Guise JA, Bloch DA, et al. Reliability of a quantification imaging system using magnetic resonance images to measure cartilage thickness and volume in human normal and osteoarthritic knees. Osteoarthr Cartilage 2003;11:351–60.

[36] Recht MR, Disler DG, editors. MRI of Cartilage. New York: Thieme; 2001.

[37] Roberts S, Weightman B, Urban J, Chappell D. Mechanical and biochemical properties of human articular cartilage in osteoarthritic femoral heads and in autopsy specimens. J Bone Joint Surg Br 1986;68:278–88.

[38] Samosky J. Spatially-localized correlation of MRI and mechanical stiffness to assess cartilage integrity in the human tibial plateau. PhD Thesis, Harvard-MIT Division of Health Sciences and Technology, Massachusetts Institute of Technology, 2002.

[39] Tiderius CJ, Olsson LE, Leander P, Ekberg O, Dahlberg L. Delayed gadolinium-enhanced MRI of cartilage (dGEMRIC) in early knee osteoarthritis. Magn Reson Med 2003;49:488–92.

[40] Trattnig S, Mlynarik V, Breitenseher M, Huber M, Zembsch A, Rand T, et al. MRI visualization of proteoglycan depletion in articular cartilage via intravenous administration of Gd-DTPA. Magn Reson Imaging 1999;17:577–83.

[41] Treppo S, Koepp H, Quan EC, Cole AA, Kuettner KE, Grodzinsky AJ. Comparison of biomechanical and biochemical properties of cartilage from human knee and ankle pairs. J Orthop Res 2000;18:739–48.

[42] Vasara A, Nieminen MT, Peterson L, Lindahl A, Jurvelin JS, Kiviranta I. In vivo assessment of autologous chondrocyte transplantation using arthroscopic stiffness measurement and quantitative MRI of proteoglycans. In: Trans Orthop Res Soc, Dallas, 2002.

[43] Wayne JS, Kraft KA, Shields KJ, Yin C, Owen JR, Disler DG. MR imaging of normal and matrix-depleted cartilage: correlation with biomechanical function and biochemical composition. Radiology 2003;228:493–9.

[44] Williams A, Gillis A, McKenzie C, Po B, Sharma L, Micheli L, et al. Glycosaminoglycan distribution in cartilage as determined by delayed gadolinium-enhanced MRI of cartilage (dGEMRIC): potential clinical applications. AJR Am J Roentgenol 2004;182:167–72.

[45] Xia Y. Magic-angle effect in magnetic resonance imaging of articular cartilage: a review. Invest Radiol 2000;35:602–21.